Polymer Bulletin (2024) 81:11173–11197
https://doi.org/10.1007/s00289-024-05239-4

ORIGINAL PAPER

Development of commercially viable and high-performance upcycled plastic waste nanocomposites for automotive and electrical industry

Yasir Qayyum Gill[1] · Faiqua Jabeen[1] · Farhan Saeed[1] · Muhammad Wasif[1] · Zarq-Ullah Javed[1] · Umer Mehmood[1]

Received: 18 September 2023 / Revised: 4 March 2024 / Accepted: 11 March 2024 /
Published online: 31 March 2024

Abstract

Waste management has become a major concern due to the extensive use of commodity polymers. Nowadays, one of the most widely used commodity polymers is nonwoven PP. The extensive utilization of polypropylene produces a large amount of waste, making their upcycling and recycling the biggest challenge. This research aims to develop an economical nanocomposite by upcycling nonwoven waste for utilization in the automotive and electronic sectors. A two-step melt blending technique was used to prepare polypropylene waste/silica nanocomposites. The nanocomposites formed were characterized by their morphological, mechanical, thermal, rheological, chemical, and electrical properties. From the results, it was concluded that the optimum mechanical, thermal, and chemical resistance properties were achieved for PP-01 formulation showing a 9.95% increase in heat deflection temperature, a 27.57% decrease in the rate of burning, a 5.4% increase in shore D hardness, 26.09% increase in flexural strength, 11.6% increase in melt flow index, and 66.25% increase in solvent resistance as compared to waste polypropylene. At the same time, the best electrical results were obtained at 0.5 wt.% with a 5.36% increase in the breakdown strength. The resistance value increases from 4.67×10^{12} Ω to 2×10^{13} Ω. The overall research shows that optimum mechanical and thermal properties were achieved at 1 wt.% so that the PP-01 formulation can be used effectively for automotive applications. In contrast, maximum electrical resistance was achieved at the PP-0.5 formulation so that this formulation could be effectively used for electrical insulation applications.

Keywords Nanocomposites · Waste · Upcycling · Plastic · Automotive · Electronic

✉ Umer Mehmood
umermehmood@uet.edu.pk

[1] Department of Polymer and Process Engineering, University of Engineering and Technology, Lahore, Pakistan

Introduction

In the past few years, the nonwoven industry has been expanding rapidly while offering a large diversity of products for various applications, including hygiene, wipes for personnel care, construction, automotive, civil engineering, filtration, food, beverages, etc. [1, 2]. According to the European Disposal and Nonwoven Association (EDANA) 2020 Statistics, the European nonwoven industry grew by 7.2% to reach 3,075,615 tons (85.9 billion square meters) with an estimated turnover of €9555 million [3]. This large nonwoven industry produces huge amounts of waste, including production lines and consumer waste [1]. A significant portion of this nonwoven waste (80–90%) is disposed of by either burning or burying it, which results in the formation of harmful environmental pollutants [1, 4]. Reusing and recycling this nonwoven waste is one of the significant tasks faced by the world to reduce its environmental impact and to encourage the efficient use of resources [5]. Globally, only 1% of nonwoven waste is recycled, upcycled, or reused. The reason for their low recycling rate is that the nonwoven waste is lightweight, and different kinds of separation techniques (based on density, MFI, and solubility in specific solvents) are required to separate them into different categories [4].

The most common nonwoven consists of polyester (22.5%) and polypropylene (63%) [5, 6]. Nonwoven PP accounts for about 3.3 million metric tons of the worldwide production of synthetic nonwoven fabric. Nonwoven PP is widely utilized in personnel protective equipment such as surgical gowns, hard headwear, face masks, laboratory coats, and shoe covers, thus providing excellent protection against germs, airborne microorganisms, blood, and chemical spillage [4]. All these PPEs are the single used item used in large numbers daily in hospitals, laboratories, research centers, and clinics, accounting for a large amount of waste [7]. According to World Health Organization (WHO) report, 766,895,075 cases of COVID-19 have been confirmed by May 25, 2023 [8]. Increasing cases of COVID-19 result in the usage of a large number of PPEs as a necessary protective measure against the spread of the virus [9]. According to WHO 2020 report, during the COVID-19 pandemic, a 40% increase in the manufacturing of disposable personnel protective equipment was observed. This increment in the usage of personnel protective equipment also results in rapid disposal, thus affecting the environment [10]. According to an estimate, during COVID-19, one twenty-nine million facemasks and sixty-five million gloves polluted the environment in one month [11]. During the first year of COVID-19, it was estimated that 3,500,000 metric tons of the nonwoven polypropylene mask waste had been discarded in landfills, resulting in a 3.5% increment in global municipal solid waste [12]**.** Currently, recycling programs do not include synthetic textiles or nonwoven fabric. Therefore, PP waste is directly disposed of by burning or burying it. Both these methods of disposing of nonwoven PP waste led to environmental pollution [6]. These practices also result in a significant economic loss because this waste can be used to produce multifunctional materials due to the presence of a wide variety of valuable additives [4]**.**

Various studies have been done on producing a cost-effective and efficient product using nonwoven fabric. Fiber-reinforced polymeric matrices are

widely used in applications that require better mechanical properties, such as automobiles, aerospace, and aircraft. Nonwoven polypropylene waste composites can be an excellent material for such applications. Only a few studies are available in the literature on the recycling or upcycling of nonwoven PP waste in composite [1]. Ching-Wen Lou et al. recycled polypropylene and polyester nonwoven selvages to develop composites with sound absorbent capability. Results showed that porous composites exhibit excellent absorption performance for high-frequency sound waves (especially frequencies greater than 2000 Hz) [5]. In another study, Ching-Wen Lou et al. recycled nonwoven PP waste selvages to manufacture conducting fibers and studied their surface resistivity and electromagnetic shielding effectiveness [13]. Claudia A Echeverria et al. developed nontoxic thermoplastic–lignocellulose hybrid sheet materials for construction and building applications using recycled nonwoven PP as a matrix phase with dispersed wood fibers as the reinforcement [14]. Ayman Nafaday et al. prepared nonwoven PP waste nanocomposites by adding $AgNO_3$ and aniline into the plasma-pretreated nonwoven PP matrix with electroconductive, superhydrophobic, and antimicrobial properties [15]. Pattaraporn Singsatit and Vimolwan Pimpan used nonwoven fabric waste obtained from the medical gown manufacturing process and used them as a filler in HDPE [16]. Battegazzore et al. mechanically recycled medical face masks by melt blending them in an extruder at a high temperature, and their mechanical, thermal, and thermomechanical properties were studied [17]. Jia et al. produced a composite geotextile using nonwoven PET and PP selvages. A sandwich structure was prepared by using two layers (top and bottom) of nonwoven polyethylene terephthalate that encloses recycled PP selvages and nylon geogrid [18].

Only a few studies are available on the recycling of nonwoven polypropylene waste by incorporating nanofillers. Nonwoven polypropylene fabric-based nanocomposites can be widely used as thermal insulation, electrical insulation, and fireproof layers due to their affordability, lower processing costs, good processability, excellent insulation properties, good chemical resistance, almost no water adsorption, and widespread accessibility [19]. Therefore, this research mainly focuses on the using nanofillers to upcycle nonwoven PP-based personnel protective equipment waste. Nowadays, one of the most commonly used nanofiller is silica. SiO_2 nanoparticles are a specific form of colloidal metal oxide with a polymeric structure composed of siloxane (Si–O–Si–O) structures and silanol (Si–OH) groups on the surface. Numerous studies have been conducted to study the properties of silica and its potential uses in advanced technologies, such as nanotechnology, advanced materials, composites, and nanostructures. Silica is also being investigated for its potential applications in environmental remediation, wastewater treatment, and renewable energy production. M.A. Batiha et al. have developed a nontoxic polyvinylpyrrolidone (PVP)-propylmethacrylate–silica nanocomposite to efficiently adsorb lead, copper, and nickel cations from contaminated wastewater. They synthesized silica nanocomposites from rice straw residues, activated the surface with (3-aminopropyl) triethoxysilane and 3-(trimethoxysilyl) propyl methacrylate (VNH_2–SiO_2), and exploited acrylates group to link the vinylpyrrolidone monomer to produce a nontoxic polyvinylpyrrolidone–propyl methacrylate–silica nanocomposite (PVP–SiO_2). It was found from the results that

PVP-SiO_2 exhibits fast adsorption rates and good adsorption capacity of 142.8, 111, and 46.08 mg/g, toward lead, copper, and nickel cations, respectively, compared to VNH_2–SiO_2 [20]. Cobley et al. studied the effect of low-frequency (20 kHz) pulsed and continuous ultrasound on the gold plating of silica nanoparticles for use in composite solders [21]. Danhua Xie et al. developed an ethanol gel as a hand sanitizer using chitosan and silica nanoparticles. The gel showed high antibacterial activity. It was concluded from the research that stable gels were formed by using chitosan as a gelling agent in high ethanol concentration (up to 80%) in the presence of silica nanoparticles [22].

Likewise, when silica nanoparticles were used as a filler in nonwoven PP they give nonwoven PP excellent mechanical properties and thermal, chemical, and electrical stability due to its high thermal stability, electrical insulation, large pore volume, and large surface area [23]. Also, a substantial increase in the properties can be observed by adding varying loadings of silica nanoparticles in nonwoven polypropylene matrix. This research aims to study the effect of the silica nanofiller on the mechanical, thermal, chemical, and electrical properties of nonwoven PP waste. Various techniques can be used to manufacture polypropylene waste-based nanocomposites, such as melt blending, in situ polymerization, and solution blending [24]. The melt blending technique is normally performed using an internal mixer or an extruder. The extent to which the dispersion and distribution of silica filler occur mainly depends on the nature and type of the mixing motion. Also, this technique has been found to be more economical than other methods used for manufacturing nanocomposites [25–28]. Therefore, in this research melt blending technique was preferred to avoid the formation of agglomerates in the polypropylene matrix and to make economic nanocomposites. Other methods that can be used to avoid agglomeration include ultrasonication of nanofiller, incorporation of coupling agents, changes in processing conditions, and equipment modification. The method used in the research combines melt blending with ultrasonication using a single screw extruder. This method is beneficial compared to the methods used in the previous studies as it eliminates the water from the mixture or enters the extrude, making it also suitable for hygroscopic materials [4]. Another advantage of using the melt blending technique is that it does not require any solvent during the manufacturing of the nanocomposite, as used in the case of solution blending [29]. Originally, the properties of the nanocomposite depend on the structure formed after the mixing of the filler in the polymer matrix [28, 30].

The nanocomposites formed during this research have been characterized by their morphological, mechanical, thermal, rheological, chemical, and electrical properties. Various tests such as Charpy impact strength, heat deflection temperature, flammability tests, breakdown strength, four-probe and tera-ohm resistance test, important for automotive and electrical applications, have been performed and reported in the paper.

Experimental

Material

Nonwoven polypropylene (PP) was collected by Multi Solutions Private Limited, Lahore, Pakistan. Nonwoven fabric waste of 40 gsm (gram per square meter) is manufactured by the melt spun-bond technique and was provided by Multi Solutions Private Limited, Lahore, Pakistan. Silica with a commercial name of ULTRASIL® VN 3 GR, particle size ranging between 20 and 54 nm, was obtained from Evonik, Germany.

Sample preparation

Nonwoven fabric was disassembled manually to isolate fabric portions. The material was separated into two fractions based on visual inspection, i.e., nylon fabric and polypropylene fabric. Then, to get rid of dirt, the nonwoven polypropylene fabric was thoroughly cleaned with a mild detergent solution and subsequently with distilled water. Thereafter, the whole material was then dried at ambient temperature for 48 h. For further drying of nonwoven polypropylene fabric, it was kept in the oven for 24 h at 100 °C.

Methodology

Nonwoven polypropylene fabric waste was compression molded for 10 min at 180 °C and 200 bars of pressure using a laboratory-scale compression molding machine (Gibitre Instrument Srl, model: Laboratory press). In the first stage, sheets produced by the compression molding method were subjected to mechanical size reduction to obtain coarser particles using a shredder (Medina Engineering Works Pvt. Ltd. Lahore, Pakistan, model: SH014). In the second stage, a grinder (Royal Catering™ Multi grinder, model: RCMZ1000) was used to finely micronize the larger fragments into smaller particles. To distinguish between smaller and larger particles, the resultant powder was sieved. The coarser particles were again subjected to grinding to make them smaller.

The silica nanofiller was then ultrasonicated at room temperature for 1 h using Stalwart Ultrasonicator, model: S-DS-3, in an aqueous medium (water) at a frequency of 40 kHz. An aluminum container (having an 11 L capacity) was kept on a heat source, and PP powder and water were added. The mixture was continuously stirred using an electric overhead stirrer. When the mixture begins to boil, sonicated silica in an aqueous medium was added into it, and the lid was fastened. This mixture was then heated for fifteen minutes at 110 °C and 30 psi pressure. The resulting polypropylene and silica slurry were then stored in the laboratory at ambient temperature for about two weeks to eliminate water content. Polypropylene powder was then thoroughly dried for an additional 5 h at 80 °C in an electric

oven (Laboratory dry oven, model: DHG-9053). Then the polypropylene powder and silica mixture was melt-blended using a laboratory-scale extruder (Medina Engineering Works Pvt. Ltd. Lahore, Pakistan, model: SSE010). The extruded was equipped with a screw having the diameter of 4.5 cm, length 75 cm and a rotational speed of 62 revolution per minute. Extruder was powered by an electric motor of 10 horsepower. The temperature used for the blending of the polypropylene powder and silica mixture ranges from 210 to 230 °C (temperature varies 10 degrees for each zone, i.e., 210 °C for feeding zone, 220 °C for compression zone and 230 °C for the metering zone of the extruder). Extruded melt was then cooled at ambient temperature. Specifications of all samples are shown in Table 1.

A size reduction procedure utilizing a shredder and a grinding mill was then used to grind extrudate. Sheets were then compression molded for 8 min at about 200 °C and 200 bars pressure using laboratory-scale compression molding (Gibitre Instruments, model: Laboratory press). After compression molding, the samples were rapidly moved to a second water-cooled laboratory-scale compression molding machine (Medina Engineering Works Pvt. Ltd. Lahore, Pakistan, model: M150) to cool the sheets for 10 min. The resultant square sheets were then cut into the appropriate 3- to 4-mm-thick sample sizes to perform various characterization techniques. Figure 1 shows the schematic of the methodology used for this research.

Characterization

Morphological analysis

Fourier Transform Infrared Spectroscopy (FTIR) was performed using JASCO™ FT/IR 4600 with 32 scans to study the composition of the waste polypropylene and the changes that appeared after adding silica nanofiller in nonwoven polypropylene waste. The FTIR apparatus was operated in transmission mode, with a spectral range between 400 and 4000 cm^{-1}. To observe the distribution/dispersion of SiO_2 nanofillers in the PP matrix at the microscopic level, *optical microscopy* of the filled and unfilled samples was conducted. To prepare the samples

Table 1 Specifications of the sample prepared

Samples	Wt.% of silica	Total weight of sample (g)	Amount of silica (g)	Amount of PP (g)	Ultrasonication time of SiO_2 (min)
W-PP	0	250	0	250	60
PP-0.25	0.25	250	0.625	249.375	60
PP-0.5	0.5	250	1.25	248.75	60
PP-0.75	0.75	250	1.875	248.125	60
PP-01	1	250	2.5	247.5	60
PP-02	2	250	5	245	60

W-PP: waste polypropylene; PP: polypropylene; SiO_2: silica

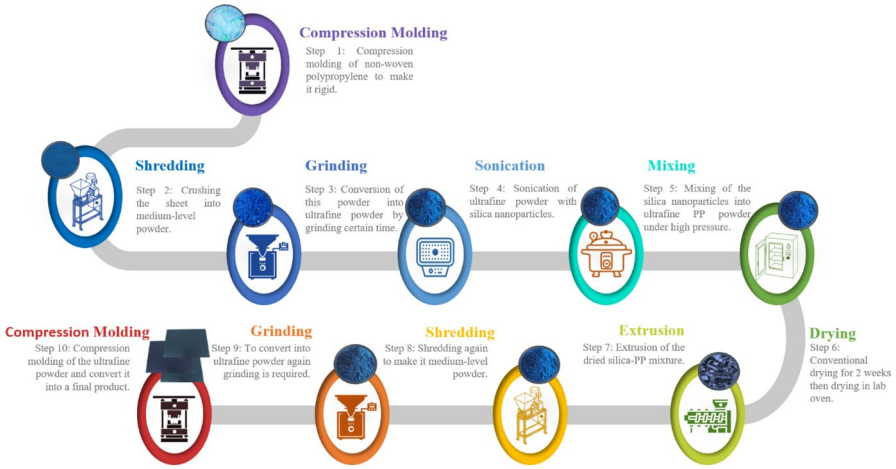

Fig. 1 Schematic representation of the methodology used for the research

for optical microscopy, the hot plate method was used. Firstly, a glass slide was carefully positioned on the hot plate, with the temperature set at 180 °C. From each unique formulation, a small sample was obtained and placed onto the slide. Once the sample began to melt, it was gently pressed against the slide to obtain as minimum thickness as possible.

Thermal analysis

Shimadzu™ TGA-50 was used to determine the *thermal stability* of samples according to ASTM-E2550. The test was performed in the nitrogen atmosphere using a temperature increase from 50 to 600 °C and a heating rate of 10 °C/min. *Heat deflection temperature (HDT)* of the filled and unfilled PP waste/silica samples was carried out according to the ASTM-D648 using GOTECH™ HV-2000- M3M Vicat/HDT tester. The test was repeated three times on three different specimens taken from each sample. A total of 418-g weight was applied to the sample during the test. A test was conducted to study *softening point, melting point, and degradation temperature* of filled and unfilled samples on Ats Faar Industries SRL Melting point apparatus. *UL-94 flammability test* was carried out to study the flammability characteristics of silica-filled polypropylene nanocomposites. A horizontal flame test was performed for each sample according to ASTM-D635. The burning rate was measured according to Eq. 1 [31]**:**

$$V = {}^{60L}\!/_{t} \tag{1}$$

where V = linear burning rate, L = burned length in millimeter, and t = time required for burning in seconds.

Mechanical analysis

The *Shore D hardness* of the samples was measured using a Gibitre Instruments digital manual hardness meter. *Charpy Impact test* of samples was performed using GOTECH-7045-HMH Pendulum Impact tester. Three samples from each formulation were tested according to ASTM D6110. The *flexural test* was carried out according to the ASTM-D790 using the universal testing machine TRA test 2810. The flexural strength and flexural modulus of the three samples from each formulation were measured using Eqs. 2 and 3 [4]**:**

$$\text{Flexural strength} = {}^{3PL}/_{2bd^2} \tag{2}$$

$$\text{Flexural modulus} = {}^{L^2m}/_{4bd^2} \tag{3}$$

where P = extreme value of the load on the curve, L = length of support span, b = width, d = depth of the samples, and m = slope of the tangent, respectively.

Chemical testing

A *solvent immersion test* was performed to study the chemical stability of the formed nanocomposites. For the solvent immersion test, one sample from each formulation was cut (1×1 in^2) and then weighted using a precision balance (that can measure in the range of 0.1 g to 500 g). These samples were then placed in the conical flask containing 10ml of solvent, i.e., methyl ethyl ketone (MEK). Flask was then covered with aluminum foil at room temperature for 68 h. After 68 h, swollen samples were taken out from the solvent and the excess solvent was removed from them using a short contact filter paper. These swollen samples were then again weighed, and the weight gain was determined using Eq. 4 [32]**,** given below.

$$\text{Weight gain (\%)} = {}^{(m_2 - m_1)}/_{m_1} \times 100 \tag{4}$$

where m_1 = mass of the sample before swelling and m_2 = mass of the sample after swelling.

The *density test* was conducted by using KAREN™ ARS 120-4 density meter, according to the ASTM 792D. Density was measured using toluene in a 200-ml glass beaker. Measurements were taken according to Archimedes' principle and were repeated five times for each formulation.

Electrical properties

A *dielectric breakdown test* was performed using high-voltage equipment. One sample having the dimensions of 3×3in was cut from each formulation and placed between the electrodes. The voltage is gradually increased until

the breakdown occurs. The maximum voltage at which breakdown occurs is then divided by the thickness of the samples to obtain dielectric strength [31]. *Resistance measurements* were carried out on CEAST TOA/I Tera-Ohm meter (Type: 6148) using disk shape samples (One sample from each formulation). From resistance, conductance, resistivity, and conductivity were calculated using Eq. (5), Eq. (6), and Eq. (7), respectively.

$$\text{Conductance} = {}^{1}/_{R} \tag{5}$$

$$\text{Resistivity} = {}^{RA}/_{L} \tag{6}$$

$$\text{Conductivity} = {}^{1}/_{\rho} \tag{7}$$

where R = resistance, A = area of the disk, L = length of the disk, and p = resistivity of the samples at 1000 V.

The *electrical conductivity* of the samples was studied using a four-probe meter with 0.2 cm spacing between each probe. One sample from each formulation having dimensions of 1×1 cm^2 was used to perform the test. The voltage was measured by applying the current between the external terminals. Voltage and current values are used to calculate resistance. Resistance is measured using Eq. 8 [33]:

$$V = \text{IR} \tag{8}$$

To calculate resistivity, Eq. 9 is used:

$$\text{Resistivity} = R \cdot t \tag{9}$$

where R = resistance and t = thickness of the sample. For sample thickness 40% greater than the probe spacing, a correction factor of 0.6336 is applied [34].

Rheological properties

KARG Industrietechnik™ Melt Flow Tester was used to measure the sample's *Melt Flow Index (MFI)* according to the ASTM D1238. MFI analysis was performed to examine the effect of filler loading on the processing and flow behavior of the melt. Powder of polypropylene-based sample weighing five grams at 230° C was filled in the barrel, and a load of 2160 g was applied to the piston to determine their melt flow rates. The MFI of the sample was measured according to Eq. 10:

$$\text{MFI}_{(\text{T,w})} = (\text{M} \times 600)/\text{t} \tag{10}$$

where T = barrel's temperature, w = load applied to the piston in kilograms, M = extrudate's weight in grams, and t = time in minutes it took for the extrudate to flow through the barrel.

Result and discussion

Morphological analysis

Fourier transform infrared spectroscopy analysis

The FTIR spectrum of nonwoven PP (W-PP) is in the range of 500–4000 cm^{-1}, as shown in Fig. 2a. The peak at 2917 cm^{-1} corresponds to the asymmetrical stretching of CH_2 [35]. The peak at 2838 cm^{-1} corresponds to the stretching of CH. The peaks at 1455 cm^{-1} and 1373.07 cm^{-1} are assigned to the asymmetric and symmetric bending of the CH_2 and CH_3 groups [4]. The peaks at 1251.58 cm^{-1} and 1100.19 cm^{-1} are related to the C-H bending, wagging, and CH_3 rocking [35]. Peak located at 843.704 cm^{-1} is assigned to the C-CH_3 stretching, vibration, and CH rocking. The peaks in the range of 800–1550 cm^{-1} and 2900–2700 cm^{-1} are the distinctive peaks of nonwoven PP waste [4, 36].

FTIR spectrum of PP waste/silica nanocomposites is shown in Fig. 2b. Two distinctive peaks can be observed in the case of PP/silica nanocomposites. The peak at 1733 cm^{-1} corresponds to the C=O stretching due to the oxidation of the W-PP during processing [37] while another peak at 973 cm^{-1} was also observed. This peak attributes to the Si–O– group vibration because of the formation of the Si–O bond with the carbon atom (–C) of the PP, thus conforming to the presence of silica in the PP [38, 39]. Based on studies, Oh. Teresa explains that in the FTIR spectrum of silica, the Si–O–Si bonds are visible at approximately 970 cm^{-1}. When silica is added to PP, it forms a bond between the carbon chain of the polypropylene and the Si–O–Si bond of silica, resulting in the formation of a Si–O–C bond where one of the Si atoms from Si–O–Si bond is replaced by a carbon atom. And thus Si–O–C bonds are visible in the range of 950–1150 cm^{-1} [40]. This bonding will restrict the chain movement making them stiffer and

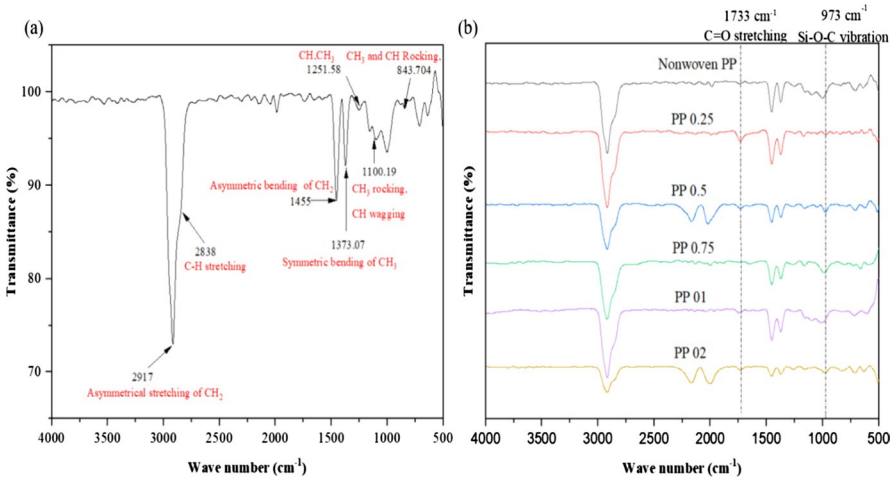

Fig. 2 FTIR spectrum of **a** nonwoven PP waste, **b** nonwoven PP waste consists of different silica loading

leading to an overall increase in nonwoven PP waste's mechanical and insulation properties.

Optical microscopy

To enhance the properties of the nonwoven polypropylene via the addition of silica, it is necessary to get homogenous dispersion and distribution of the reinforcement in the matrix. Optical microscopy of the samples was conducted to study the dispersion and distribution of silica nanoparticles in the PP matrix at the microscopic level. Another important objective of optical microscopy is to understand the reinforcement phenomena of filler in the matrix and the effect of aggregation of the fillers on the properties. Figure 3 shows the OM micrographs of W-PP and PP/silica nanocomposite samples at 50× resolution. It can be seen from micrographs that silica nanoparticles are homogenously dispersed in the samples. However, agglomeration can be observed in the case of PP-0.25 and PP-02 formulations. These aggregates are shown in Fig. 3 by making a white circular pattern around them. These agglomerates are the characteristic of nanofiller formed due to the van der Waals interaction between nanoparticles. In the case of PP-0.25, agglomerates may be due to the poor ultrasonication of the silica that leads toward poor dispersion of nanoparticles in the polymer matrix. In contrast, at higher silica loading, the agglomeration is attributed to the increased ability of the SiO_2 particles to form aggregates at higher loadings and to the poor interaction of silica with polymer matrix during melt blending. Therefore, to effectively reinforce the nanofiller into a polymer matrix, one must optimize the inherent characteristics of the nanofiller in dispersion and nanoscale morphology.

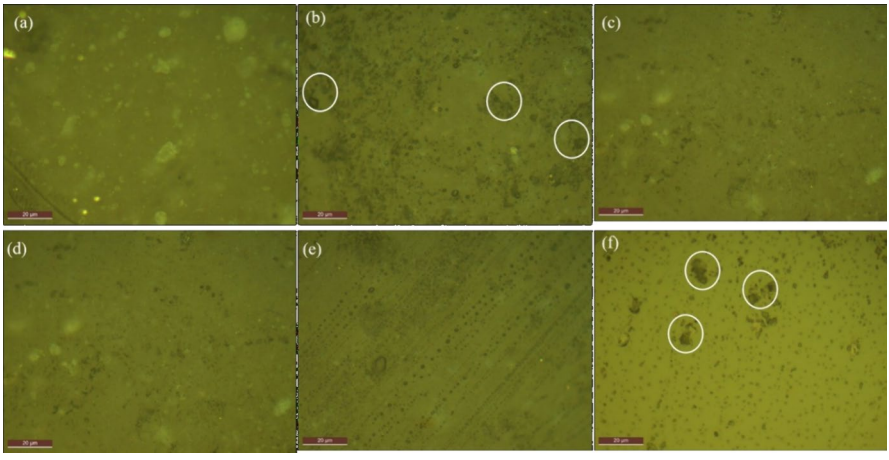

Fig. 3 Optical microscopy analysis of **a** W-PP, **b** PP-0.25, **c** PP-0.5, **d** PP-0.75, **e** PP-01, **f** PP-02

Mechanical analysis

Shore D hardness testing

Hardness is defined as the ability of the material to withstand indentation/deformation. It is a quasi-mechanical property that affects the final properties or applications. The hardness of the nonwoven polypropylene waste and its samples is shown in Fig. 4a. An increasing trend in the hardness of the nanocomposites was observed with a 6.7% rise in the hardness at 2 wt.% of silica as compared to W-PP. A similar increasing trend of hardness in the case of silica nanocomposites has been observed in the literature. Safaa A Al-Shawi et al. observed a 3.2% increase in the hardness of the epoxy matrix by adding 2 wt.% of silica [41]. Luyt et al. found a 30.3% increase in the hardness of polycarbonate with the addition of silica nanoparticles [42]. Similarly, Nadia A. Ai et al. observed a 60% increase in the hardness of nanoreinforced silica–epoxy composites [43]. The increase in Shore D hardness of nanocomposites can be ascribed to the better cross-linking and stiffness of backbone chains. An

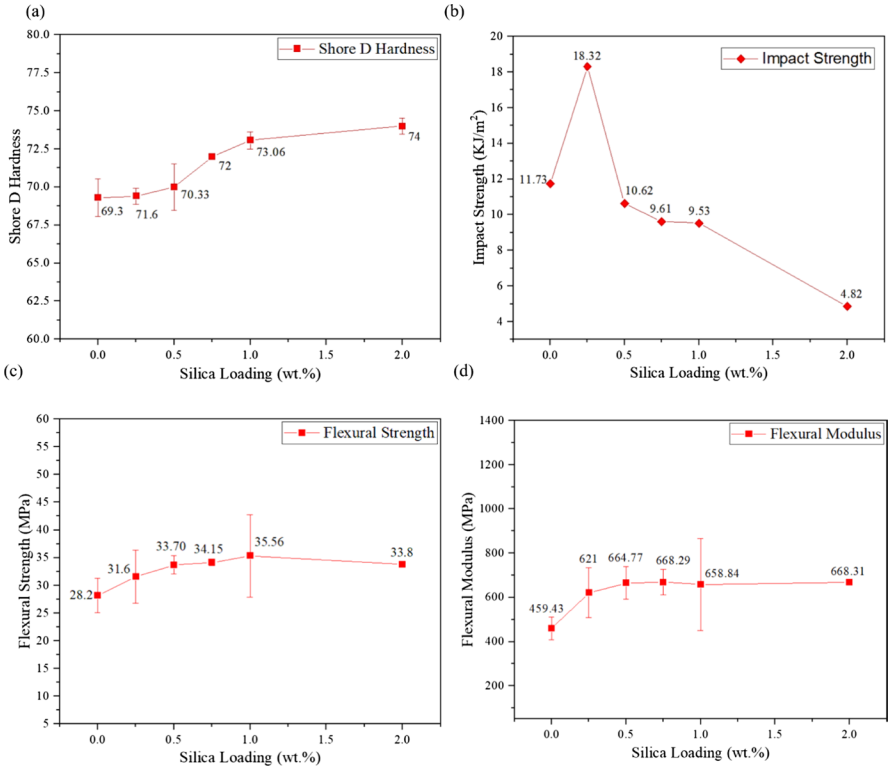

Fig. 4 **a** Effect of silica loading on the Shore D hardness of nonwoven PP. **b** Effect of silica loading on the Charpy Impact strength of nonwoven PP. **c** Effect of silica loading on the flexural strength of nonwoven PP. **d** Effect of silica loading on the flexural modulus of nonwoven PP

increase in hardness will directly affect nanocomposite's strength, modulus, abrasion, and scratch resistance [42].

Charpy impact test

Impact resistance is an important mechanical property of a material that determines its ability to withstand a sudden applied load. The results of the Charpy impact test for all samples are shown in Fig. 4b. The highest value for Charpy impact strength was observed for the lowest weight percentage of nanoparticles in the PP matrix, i.e., 0.25 wt.% showing a 56% enhancement in the strength as compared to the waste polypropylene sample. After this, the maximum absorbed energy continuously decreases with the lowest value of 4.82 kJ/m^2 at 2 wt.% as compared to W-PP (11.73 kJ/m^2). The enhancement in impact strength could be due to the presence of an interconnected silica network at low weight percentages, which reinforces the material primarily through hydrogen bonding [42, 44]. At high loadings of nanoparticles, polymers' ductility was reduced, leading to lower impact absorption energies [45].

Feng Yang et al. reported a similar result for PA6/modified silica nanocomposites, where a 7% improvement in the impact strength was observed at 5 wt.% of the silica, and then, a continuous decrease was observed with the increasing silica loading [46]. A similar trend in the impact strength of polycarbonate/silica nanocomposites was also studied by Luyt et al. where an almost 30% increase in the absorbed energy was observed on the incorporation of 1 wt.% of aerosol-90 silica, followed by a decreasing trend on the further addition of silica into the polycarbonate [42].

Flexural strength

Flexural strength is the combination of both compressive and tensile strength. Therefore, the flexural properties of nanocomposite depend on both reinforcement and matrix. Figure 4c and d shows the flexural strength and modulus of the PP/silica nanocomposite, respectively. The flexural strength increased by 12.05, 19.50, 21.09, 26.09, and 19.85% for PP-0.25, PP-0.5, PP-0.75, PP-01, and PP-02 samples, respectively, compared to the W-PP. The maximum flexural strength value was observed for the PP-01 sample, which is 35.56 MPa. After that, the flexural strength decreases. Flexural modulus also shows 35.1%, 44.69%, 45.4%, 43.40%, and 45.46% improvement for PP-0.25, PP-0.5, PP-0.75, PP-01, and PP-02 samples, respectively, compared to the waste PP. The maximum value of flexural modulus was observed for the PP-0.75 and PP-02 samples, i.e., almost 668 MPa. The improvement in the flexural properties may be due to the better filler and matrix interaction of PP and silica (reinforcing effect of silica) and also to the fact that the addition of the silica improves the energy absorption mechanism during compression [4, 47]. The decrease in flexural properties at higher silica content could be attributed to the enhanced ability of the SiO_2 to form agglomerates at higher loadings [48].

Thermal analysis

Melting point test

A melting point test was performed to study the behavioral changes of the nonwoven PP waste and its nanocomposites with respect to temperature. The pictorial representation of behavior when exposed to high temperatures is shown in Fig. 5.

The values obtained during tests are reported in Table 2. An overall increasing trend was observed showing the heat stability of polypropylene on the addition of silica. The data shown in the table also give information about the processing temperatures. The processing temperature is theoretically 30–40 °C above the melting point. Therefore, the processing temperature of all samples can easily be predicted using the information related to the melting point.

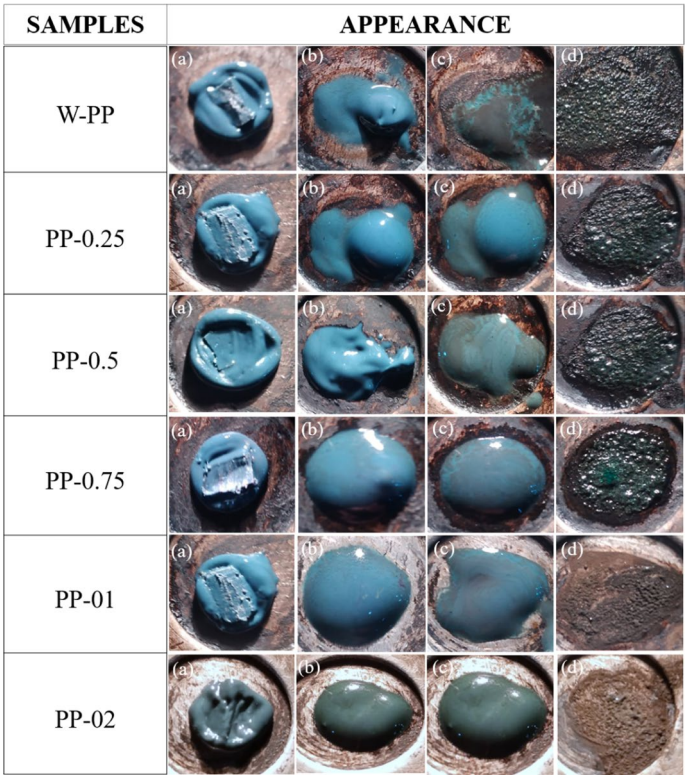

Fig. 5 Behavior of nonwoven PP and its nanocomposites when exposed to high temperature. **a** Appearance at softening point. **b** Appearance at melting point. **c** Color change. **d** Appearance at degradation temperature

TABLE 2. Melting behavior of nonwoven PP waste and its nanocomposites

Stages	Temperature ranges (°C)					
	W-PP	PP-0.25	PP-0.5	PP-0.75	PP-01	PP-02
Softening	105	106	106	106	107	104–107
Melting	115	120	123	126	130	120–130
Color change	177	165	169	175	180	189
Bubbling	205	215	215	215	223	225
Degradation	234	240	249	254	255	250

W-PP: waste polypropylene; PP: polypropylene

Flammability test

There are various applications in polymers where flame retardancy is required, like in electronic applications. So, the fire-catching or burning properties are studied before implementing the application. All samples were tested for their burning characteristics; the results are reported in Table 3. From the results, it can be concluded that the addition of the nanosilica increases its flame resistance. All the nanocomposite samples were found to have an HB rating as the flame front approaches the 100mm reference mark and the burning rate is less than 75 mm per minute. The lowest burning rate was observed for the PP-01 sample, i.e., 18.86 mm/min, compared to 26.04 mm/min for the W-PP sample. This burning rate decline can be assigned to the silica's thermal stability, which serves as a barrier between O_2 and flame. Char formation was observed while performing the test, which acts as a barrier to oxygen and thus decreases its burning rate [4, 49]. Similar results have been found in the literature. Paulina Jakubowska et al. observed a 30.4% decrement in the linear burning rate of polypropylene by adding only 5% of the silica [50]. YQ Gill et al. reported a 65% decrease in the burning rate by adding 5% silica in the XLPEs [51]. The overall burning behavior (flame ignition, propagation, and dripping) of the samples is shown in Fig. 6.

Thermal gravimetric analysis

TGA was performed to observe the thermal stability of nanocomposites and the effect of varying filler loading on the thermal degradation of nanocomposites. An overall improvement in the degradation temperature was observed on adding silica nanofiller. Figure 7a shows the single peak thermograms obtained from the thermal gravimetric analysis, whereas Fig. 7b shows the derivatives of TGA curves that give information about the inflection points. Figure 7a and b shows that the maximum value for degradation temperature is observed for PP-0.25 formulation, i.e., 13.46° C increase in the degradation temperature compared to W-PP, also shown in Table 3. The maximum value at 0.25 wt.% of silica is attributed to the better distribution of the SiO_2 in the matrix. According to the studies, degradation temperature is highly dependent upon the distribution of the

Table 3 Chemical, rheological, and thermal properties of nonwoven PP waste and its nanocomposites

Sample	Chemical properties		Rheological properties	Thermal properties			
				HDT °C	TGA	Flammability	
	Density Kg/m^3	Solvent uptake %	MFI (g/10 min)		Degradation temperature °C	UL-94	Rate of burning mm/min
W-PP	929.76 ± 3.24	8	32.78	82.1 ± 2.68	377.51	HB	26.04
PP-0.25	931.35 ± 1.74	5.6	20.67	86.5 ± 0.7	390.97	HB	22.47
PP-0.5	934.57 ± 3.71	5.37	36.37	86.7 ± 0.42	373.24	HB	20.47
PP-0.75	935.83 ± 0.29	3.84	46.25	89.2 ± 0.28	388.97	HB	19.73
PP-01	938.36 ± 3.59	2.7	36.6	91 ± 0	368.82	HB	18.86
PP-02	930.32 ± 5.1	2.08	40.69	96.8 ± 0.42	377	HB	21.2

W-PP: Waste polypropylene; MFI: Melt Flow Index; HDT: heat deflection temperature; TGA: thermogravimetric analysis; HB: horizontal burning

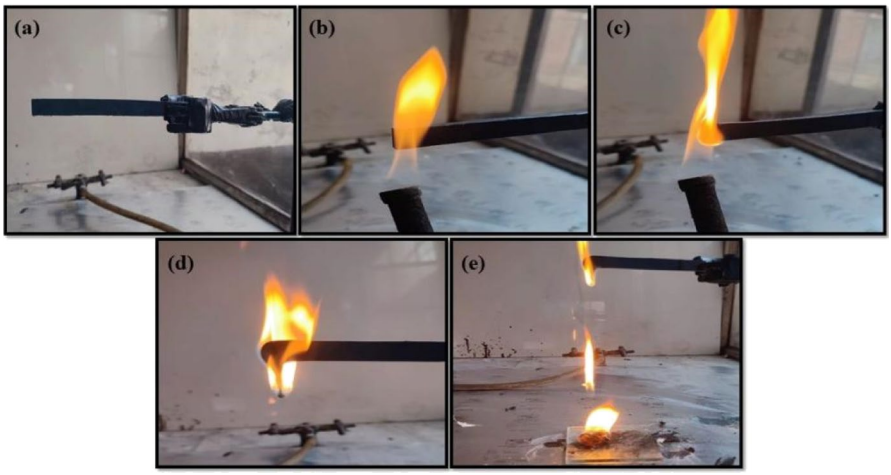

Fig. 6 Horizontal Flame test. **a** Flame test setup. **b** Ignition (igniting the bar through burner at 45 °C. **c** Propagation. **d** Dripping of melt. **e** Ignition point on a cotton swab and char formation

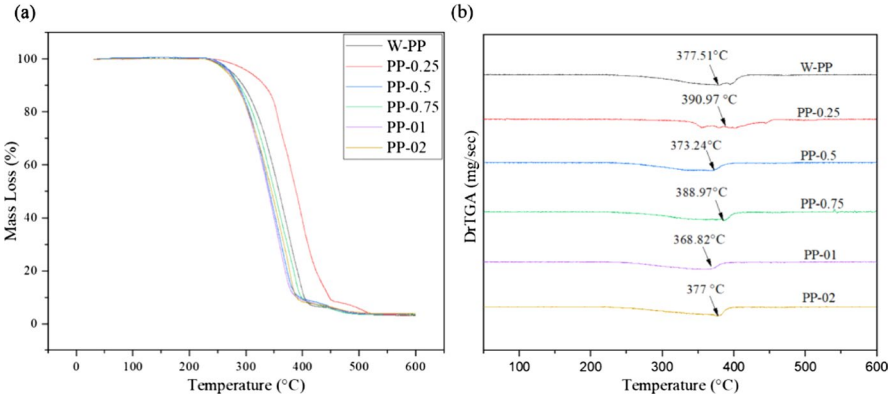

Fig. 7 Thermograms of **a** unfilled and filled silica nanocomposite samples, **b** derivative of the TGA curves

silica in the matrix; the greater the restriction for chain movement, the higher the degradation temperature will be [52]**.** Thus, the degradation temperature indicates the interfacial interaction between the filler and the matrix. At higher loadings, such as 1 and 2 wt.% degradation temperature will decrease due to the formation of agglomerates in the samples, leading toward the better particle–particle interaction of silica as compared to the silica–matrix interaction and hence decreasing its degradation temperature to the point that is almost similar to the degradation temperature of the waste–PP matrix [4, 53]**.**

Heat deflection temperature

The temperature at which a given degree of deflection occurs in a polymer bar under conditions of the constant load is known as the heat deflection temperature. HDT is found to be an important property for polymer nanocomposites to be used in the automotive industry [54]. The heat deflection temperature of W-PP and its nanocomposites are shown in Table 3. Overall an increasing trend is observed for PP nanocomposites. The highest heat deflection temperature was shown at 2 wt.% with a rise of almost 14.6° C in HDT as compared to the reference material. The increase in HDT is attributed to the better filler–matrix interaction that leads to the cross-linking of chains, causing an increase in stiffness and hence increasing its heat deflection temperature [50].

Rheological properties

Melt flow analysis

Melt flow rate is the flow of polymer melt in grams/10 min. It is the flow through an orifice, or a specific diameter die with specific pressure and temperature. Flow rate is directly related to the processing of the polymer. High molecular weight polymers are more viscous and have low MFI, which indicates the difficulty in processing [51]. MFI values of samples with various amounts of silica are presented in Table 3. An irregular trend of MFI was observed for PP/Silica nanocomposites, with the highest MFI value observed at 0.75 wt.% of silica in PP and the lowest value at 0.25 wt.% of silica, indicating a 41.09% increase and 36.9% decrease, respectively, as compared to W-PP. An increase in the MFI at a certain limit of SiO_2 in the PP is due to the molecular chain scission phenomena of the polymer (commonly shown by recycled polymers during melting) [55, 56]**.** The decrease in the MFI of the nanocomposites may be due to the percolative network that is formed between silica aggregates [55] and the better bonding of the silica with the PP and due to the better the filler interaction with the matrix, the more restrained the chains will be, and hence nanocomposites have a low melt flow index and higher viscosity [57, 58].

Chemical analysis

Solvent immersion test

A solvent immersion test was performed to examine how the cross-linking property of the nanocomposites was changed with the amount of solvent absorbed. The results of weight gain are represented in Table 3. From the results, it can be observed that the weight gain percentage is inversely proportional to the content of silica in the matrix, i.e., samples having high silica loading have less solvent uptake content than the samples having low or no silica content.

The highest weight gain, i.e., eight percent was noticed in the case of W-PP containing 0 wt.% of silica, while the lowest weight gain was observed in the case of a sample containing 2 wt.% of silica.

It can be predicted from the results that samples with more silica content generally have better cross-linking that hinders the penetration of solvent and hence low solvent uptake content [51].

Density test

Density is defined as mass per unit volume. The density measurement of the polymer samples is of great significance as it affects the mass flow rate of the polymer, which is proportional to the energy transfer data, i.e., energy transfer is related to the mass, not the volume. The density of the W-PP and its nanocomposites, as reported in Table 3. The density of nonwoven polypropylene with and without silica was observed for comparison. The density of the PP nanocomposites increases with the increasing amount of the silica except for 2 wt.%, where a decline in the value is observed. The value increases from 929.76 kg/m^3 for the W-PP sample to 938.36 kg/m^3 for the PP-01 sample, showing a 0.17, 0.51, 0.65, 0.92, and 0.06 percent increase in density at 0.25, 0.5, 0.75, 01, and 02 weight percentages of silica, respectively. In the literature, similar results have been reported, where the density increases with the increasing amount of silica in the polypropylene matrix. Tahir Ahmed and Othman Mamat reported a 37.75% increase in the density of PP with the addition of sand silica [59]. A similar trend was also studied by Hadi NJ and Mohamed DJ, where a 4.44% increase in the density of the waste polypropylene filled with silica was observed [60]. The slight improvement in the density with the increasing silica content may be due to two reasons: Firstly, silica nanoparticles have a higher density as compared to W-PP, thus causing an increase in the overall density of the nanocomposites [59]; and secondly, the density increases because increasing the concentration of the silica nanoparticles fills up the free spaces present between the PP chains [60].

Electrical properties

Dielectric breakdown strength

The dielectric BDS of the unfilled and filled polypropylene samples are reported in Table 4. Table 4 shows that the dielectric BDS increases up to a certain limit and then decreases. As compared to the W-PP sample, a 1.49%, 5.36%, 1.25%, 1.13%, and 0.53% increase in the dielectric strength of filled samples was observed at 0.25, 0.5, 0.75, 1, and 2 wt.%, respectively. The enhancement in the BDS may be due to the increase in the interfacial area. This increase in interfacial area is ascribed to the better interaction of silica nanoparticles and the polypropylene matrix leading to more entrapment of the electrons in the interaction zone (reducing the mobility and charge transfer rate) [61]. The decline in the dielectric strength could be due to

Table 4. Electrical properties of nonwoven PP waste and its nanocomposites

Sample	Dielectric BDS (kV/mm)	Four-probe conductivity (S/cm)	Tera-Ohm resistance			
			Resistance (Ohm)	Conductance (Ohm^{-1})	Resistivity (Ohm cm)	Conductivity (S/cm)
W-PP	33.39	7.78002×10^{-12}	4.67×10^{12}	2.17×10^{-13}	1.26×10^{13}	8.05×10^{-14}
PP-0.25	33.89	1.01358×10^{-11}	6.67×10^{12}	1.50×10^{-13}	1.79×10^{13}	5.58×10^{-14}
PP-0.5	35.18	1.24906×10^{-11}	2×10^{13}	5×10^{-14}	5.38×10^{13}	1.86×10^{-14}
PP-0.75	33.81	1.24348×10^{-11}	4×10^{12}	2.5×10^{-13}	1.076×10^{12}	9.29×10^{-13}
PP-01	33.77	1.10412×10^{-11}	3×10^{12}	3.33×10^{-13}	8.07×10^{12}	1.24×10^{-13}
PP-02	33.57	1.09716×10^{-11}	2.33×10^{12}	4.33×10^{-13}	6.28×10^{12}	1.61×10^{-13}

W-PP: waste polypropylene; PP: polypropylene; BDS: breakdown strength

the ability of the silica nanoparticles to form agglomerates at higher concentrations. This increase in the particle–particle interaction as compared to the particle–matrix interaction leads toward the decreasing interaction area and hence a decline in the dielectric BDS of the PP/silica nanocomposites [51].

Four-probe conductivity testing

The conductivity of PP/silica nanocomposite decreases with the increasing loading of the silica up to a certain limit and then increases. Table 4 shows the trend between the conductivity and the silica loading. From the table, it can be seen that at 0 wt.% of silica, the conductivity is 7.78002×10^{-12} S/cm. At 0.25 wt.% and 0.5 wt.%, the conductivity decreases to 1.01×10^{-11} S/cm and 1.249×10^{-11} S/cm, respectively. This decrease in conductivity is due to the insulating behavior of the silica itself. At lower loadings of the silica, there will be a better interaction between the nanosilica and PP waste. This better interaction and cross-linking will lead to increased interaction zones that restrain the motion of the electrons within the nanocomposite, lowering its conductivity. At further increasing the silica loading (1 wt.% and 2 wt.%), the silica–silica particle interaction will become more dominant as compared to the PP–silica interaction, and hence, an increase in the conductivity is observed. However, the conductivity still being less than the conductivity of the nonwoven polypropylene matrix, i.e., 1.104×10^{-11} S/cm and 1.097×10^{-11} S/cm for PP-01 and PP-02, respectively.

Tera-Ohm resistance testing

The electrical properties of the W-PP and its nanocomposites are reported in Table 4. The maximum value for resistance and resistivity is achieved at 0.5 wt.% loading of silica in PP, i.e., 2×10^{13} Ω and 5.38×10^{13} Ω. cm, respectively. Similarly, the minimum value of conductivity and conductance is achieved at PP-0.5 wt.%, i.e., 5×10^{-14} Ω^{-1} and 1.86×10^{-14} S/cm. It can be concluded from the table that up to a certain limit, there is an increase in the electrical resistance, and after that, there is a drop in the resistance, and resistivity. There is a better filler–matrix interaction, at lower percentages of silica in the PP matrix. This filler–matrix interaction provides more space for the entrapment of the electrical charges and restricts their flow through the composite. At higher silica loading, agglomeration of silica nanoparticles starts, thus enhancing the conductive behavior of the composite [62].

Conclusion

A two-step melt blending technique was introduced in the research to prepare the nonwoven polypropylene waste and silica nanocomposites. Properties of the nanocomposites were found to be dependent on the amount and dispersion/distribution of silica in the nonwoven PP matrix. FTIR spectrum confirmed the presence of silica in the nonwoven polypropylene by giving two distinctive

peaks. One at 1733 cm^{-1} corresponds to the C=O stretching, and the second peak at 973 cm^{-1} was attributed to the Si–O– group vibration due to the formation of the Si–O bond with the carbon atom of PP. OM micrographs show that silica was homogenously dispersed in the nonwoven polypropylene matrix. This distribution and dispersion of the silica causes an increase in the overall mechanical and thermal properties of nonwoven PP and also improves the nanocomposites chemical and electrical resistance. In case of thermal properties, a single peak TGA curve was observed, showing a 3.56% increase in the degradation temperature at 0.25 wt.%. Maximum heat deflection temperature was observed at 2 wt.% of silica with 14.6 $^{\circ}$ C increase in the HDT. Melting point and flammability test also confirmed the improvement in the thermal properties of the polypropylene waste on the addition of the nanosilica. An improvement in the overall mechanical properties was also observed with 56% in the impact strength, 26.09% increase in the flexural strength, and 6.78% increase in the hardness at 0.25 wt.%, 1 wt.%, and 2 wt.% of nanosilica in the polypropylene matrix, respectively. An overall increase in the electrical resistance was observed at 0.5 wt.% of the silica. These PP waste/Silica nanocomposites can be used in automotive and electronic applications such as invertor covers, engine covers, timing belts, door frames, wireless headphones and plastic smart casings etc. In the whole, it was concluded from the present research that melt blending is an economical technique that can be used for the upcycling of personnel protective equipment waste and that nonwoven polypropylene waste, on the addition of the fillers can be used as a cost-effective raw material for nonfood application.

Funding Funding for this study was received from the Pakistan Science Foundation: PSF-CRP, Grant/Award Number: PSF/CRP/3/P-UET/PPE/50.

References

1. Yalcin I, Sadikoglu TG, Berkalp OB et al (2013) Utilization of various non-woven waste forms as reinforcement in polymeric composites. Text Res J 83:1551–1562
2. EDANA (2020) Nonwoven statistics 2020. https://www.edana.org/docs/default-source/press-corner/nonwovens-statistics-2019.pdf?sfvrsn=dbad6d4c_6. Accessed 24 June 2023
3. EDANA (2021) The voice of Nonwoven. https://www.edana.org/about-us/news/2020-nonwovens-market-insights#:~:text=According%20to%20figures%20collected%20and,turnover%20of%20%E2%82%AC9%C555%20million. Accessed 24 June 2023
4. Qayyum Gill Y, Khurshid M, Mehmood U, et al (2022) Upscale recycling of nonwoven polypropylene waste using a novel blending method. J Appl Polymer Sci 139(39)
5. Lou C-W, Lin J-H, Su K-H (2005) Recycling polyester and polypropylene nonwoven selvages to produce functional sound absorption composites. Text Res J 75:390–394
6. Quintana-Gallardo A, Del Rey R, González-Conca S et al (2023) The Environmental Impacts of Disposable Nonwoven Fabrics during the COVID-19 Pandemic: Case Study on the Francesc de Borja Hospital. Polymers 15:1130
7. Overcash M (2012) A comparison of reusable and disposable perioperative textiles: sustainability state-of-the-art 2012. Anesth Analg 114:1055–1066
8. WHO Coronavirus (COVID-19) Dashboard. In: World Health Organization. https://covid19.who.int/. Accessed 24 June 2023

9. Pandit P, Maity S, Singha K et al (2021) Potential biodegradable face mask to counter environmental impact of Covid-19. Clean Eng Technol 4:100218
10. Ramasamy R, Subramanian RB (2023) Recycling of disposable single-use face masks to mitigate microfiber pollution. Environ Sci Pollut Res 30:50938–50951
11. Prata JC, Silva AL, Walker TR et al (2020) COVID-19 pandemic repercussions on the use and management of plastics. Environ Sci Technol 54:7760–7765
12. Silva ALP, Prata JC, Duarte AC et al (2021) An urgent call to think globally and act locally on landfill disposable plastics under and after covid-19 pandemic: pollution prevention and technological (Bio) remediation solutions. Chem Eng J 426:131201
13. Lou CW, Lin C-M, Hsing W-H et al (2011) Manufacturing techniques and electrical properties of conductive fabrics with recycled polypropylene nonwoven selvage. Text Res J 81:1331–1343
14. Echeverria CA, Pahlevani F, Sahajwalla V (2020) Valorisation of discarded nonwoven polypropylene as potential matrix-phase for thermoplastic-lignocellulose hybrid material engineered for building applications. J Clean Prod 258:120730
15. Nafady A, Albaqami MD and Alotaibi AM (2023) Recycled polypropylene waste as abundant source for antimicrobial, superhydrophobic and electroconductive nonwoven fabrics comprising polyaniline/silver nanoparticles. J Inorg Organ Polymers Mater 1–11
16. Singsatit P, Pimpan V (2009) Recycling of medical gown nonwoven fabric manufacturing waste as a filler for high density polyethylene. J Metals Mater Min 19
17. Battegazzore D, Cravero F, Frache A (2020) Is it possible to mechanical recycle the materials of the disposable filtering masks? Polymers 12:2726
18. Lin JH, Lin CM, Kuo CY, et al (2010) Manufacture technology of novel reinforcing composite geotextile made of recycled nonwoven selvages. In: Advanced materials research. Trans Tech Publ, pp 137–140
19. Kansal H (2016) Experimental investigation of properties of polypropylene and non-woven spunbond fabric. IOSR J Polymer Text Eng 3:8–14
20. Betiha MA, Moustafa YM, Mansour AS et al (2020) Nontoxic polyvinylpyrrolidone-propylmethacrylate-silica nanocomposite for efficient adsorption of lead, copper, and nickel cations from contaminated wastewater. J Mol Liquids 314:113656
21. Cobley AJ, Mason TJ, Alarjah M et al (2011) The effect of ultrasound on the gold plating of silica nanoparticles for use in composite solders. Ultrason Sonochem 18(1):37–41
22. Danhua Xie, Yulong Jiang, Renjie Xu, et al (2023) Preparation of ethanol-gels as hand sanitizers formed from chitosan and silica nanoparticles. J Mol Liquids 122276
23. Shirshahi V, Soltani M (2015) Solid silica nanoparticles: applications in molecular imaging. Contrast Media Mol Imaging 10:1–17
24. Amin M (2013) Methods for preparation of nano-composites for outdoor insulation applications. Rev Adv Mater Sci 34:173–184
25. Alexandre M, Dubois P (2000) Polymer-layered silicate nanocomposites: preparation, properties and uses of a new class of materials. Mater Sci Eng R Rep 28:1–63
26. Cho J, Paul D (2001) Nylon 6 nanocomposites by melt compounding. Polymer 42:1083–1094
27. LeBaron PC, Wang Z, Pinnavaia TJ (1999) Polymer-layered silicate nanocomposites: an overview. Appl Clay Sci 15:11–29
28. Tung J, Gupta RK, Simon GP et al (2005) Rheological and mechanical comparative study of in situ polymerized and melt-blended nylon 6 nanocomposites. Polymer 46:10405–10418
29. Madaleno L, Schjødt-Thomsen J, Pinto JC (2010) Morphology, thermal and mechanical properties of PVC/MMT nanocomposites prepared by solution blending and solution blending+ melt compounding. Compos Sci Technol 70:804–814
30. Dlamini D, Mishra S, Mishra A et al (2011) Comparative studies of the morphological and thermal properties of clay/polymer nanocomposites synthesized via melt blending and modified solution blending methods. J Compos Mater 45:2211–2216
31. Lim KS, Mariatti M, Kamarol M et al (2019) Properties of nanofillers/crosslinked polyethylene composites for cable insulation. J Vinyl Add Tech 25:E147–E154
32. Hirschl C, Biebl-Rydlo M, DeBiasio M et al (2013) Determining the degree of crosslinking of ethylene vinyl acetate photovoltaic module encapsulants—A comparative study. Sol Energy Mater Sol Cells 116:203–218
33. Rashid IA, Tariq A, Shakir HF et al (2022) Electrically conductive epoxy/polyaniline composite fabrication and characterization for electronic applications. J Reinf Plast Compos 41:34–45

34. Ossila. In: Four-probe method: Sheet resistance formula. https://www.ossila.com/pages/sheet-resistance-theory. Accessed 24 June 2023
35. Fang J, Zhang L, Sutton D et al (2012) Needleless melt-electrospinning of polypropylene nanofibres. J Nanomater 2012:1–9
36. Jung S, Lee S, Dou X et al (2021) Valorization of disposable COVID-19 mask through the thermo-chemical process. Chem Eng J 405:126658
37. Ajorloo M, Ghodrat M, Kang W-H (2021) Incorporation of recycled polypropylene and fly ash in polypropylene-based composites for automotive applications. J Polym Environ 29:1298–1309
38. Tan X, Xu Y, Cai N et al (2009) Polypropylene/silica nanocomposites prepared by in-situ melt ultrasonication. Polym Compos 30:835–840
39. Zoukrami F, Haddaoui N, Sclavons M et al (2018) Rheological properties and thermal stability of compatibilized polypropylene/untreated silica composites prepared by water injection extrusion process. Polym Bull 75:5551–5566
40. Oh T, Choi CK (2010) Comparison between Si–O–C thin films fabricated by using plasma enhance chemical vapor deposition and SiO_2 thin films by using Fourier transform infrared spectroscopy. J Korean Phys Soc 56(4):1150–1155
41. Al-Shawi SA, Alansari LS, Diwan AA, et al (2021) Enhancement tensile strength, creep resistance and hardness of an epoxy resin by adding SiO_2 nanoparticles. In: IOP Conference Series: Materials Science and Engineering 2021. IOP Publishing, p 012142
42. Luyt A, Messori M, Fabbri P et al (2011) Polycarbonate reinforced with silica nanoparticles. Polym Bull 66:991–1004
43. Ai NA, Hussein S, Jawad M et al (2015) Effect of Al_2O_3 and SiO_2 nanopartical on wear, hardness and impact behavior of epoxy composites. Chem Mater Res 7:34–40
44. Gustin J, Freeman B, Stone J et al (2005) Low-velocity impact of nanocomposite and polymer plates. J Appl Polym Sci 96:2309–2315
45. Sui Y, Cui Y, Cong C, et al (2022) Rheological and mechanical properties of automobile polypropylene/silica (PP/SiO_2) nanocomposites. In: Journal of Physics: Conference Series. IOP Publishing, p 012004
46. Yang F, Ou Y, Yu Z (1998) Polyamide 6/silica nanocomposites prepared by in situ polymerization. J Appl Polym Sci 69:355–361
47. Sapiai N, Jumahat A, Jawaid M et al (2020) Tensile and flexural properties of silica nanoparticles modified unidirectional kenaf and hybrid glass/kenaf epoxy composites. Polymers 12:2733
48. Zou H, Wu S, Shen J (2008) Polymer/silica nanocomposites: preparation, characterization, properties, and applications. Chem Rev 108:3893–3957
49. Motahari S, Motlagh GH, Moharramzadeh A (2015) Thermal and flammability properties of polypropylene/silica aerogel composites. J Macromol Sci B 54:1081–1091
50. Jakubowska P, Osińska-Broniarz M, Martyla A et al (2016) Thermal properties of PP-SiO2 composites filled with Stöber silica. Compos Theory Pract 6:161–166
51. Gill YQ, Ehsan H, Mehmood U et al (2022) A novel two-step melt blending method to prepare nano-silanized-silica reinforced crosslinked polyethylene (XLPE) nanocomposites. Polym Bull 79:10077–10093
52. Srisawat N, Nithitanakul M, Srikulkit K (2009) Characterizations of fibers produced from polypropylene/silica composite. J Metals Mater Miner 19
53. Sun D, Zhang R, Liu Z et al (2005) Polypropylene/silica nanocomposites prepared by in-situ sol−gel reaction with the aid of CO_2. Macromolecules 38:5617–5624
54. Wong A-Y (2003) Heat deflection characteristics of polypropylene and polypropylene/polyethylene binary systems. Compos B Eng 34:199–208
55. Dorigato A, Pegoretti A (2014) Reprocessing effects on polypropylene/silica nanocomposites. J Appl Polymer Sci 131
56. Perez-Guerrero A, Lisperguer J, Orellana F (2011) Influence of silica nanoparticles on the thermomechanical properties of recycled polystyrene. J Chil Chem Soc 56:907–910
57. Hwang S-s, Hsu pp (2013) Effects of silica particle size on the structure and properties of polypropylene/silica composites foams. J Ind Eng Chem 19:1377–1383
58. Kumar A, Patham B, Mohanty S et al (2020) Polypropylene–nano-silica nanocomposite foams: mechanisms underlying foamability, and foam microstructure, crystallinity and mechanical properties. Polym Int 69:373–386

59. Ahmed T, Mamat O (2011) The development and properties of polypropylene-silica sand nanoparticles composites. In: 2011 IEEE Colloquium on Humanities, Science and Engineering. IEEE, pp 172–177
60. Hadi NJ and Mohamed DJ (2017) Study the relation between flow, thermal and mechanical properties of waste polypropylene filled silica nanoparticles. In: Key engineering materials. Trans Tech Publ, pp 28–38
61. Abdul Razak NI, Yusoff NISM, Ahmad MH et al (2023) Dielectric, mechanical, and thermal properties of crosslinked polyethylene nanocomposite with hybrid nanofillers. Polymers 15:1702
62. Rytöluoto I, Ritamäki M, Lahti K, et al (2018) Compounding, structure and dielectric properties of silica-BOPP nanocomposite films. In: 2018 IEEE 2nd International Conference on Dielectrics (ICD) 1–5 July 2018, pp 1–4